



Molecular Crystals and Liquid Crystals

Publication details, including instructions for authors and subscription information:

<http://www.tandfonline.com/loi/gmcl20>

Liquid Crystal Filled Polymer Structure SLM Devices

Garry Lester^a & Stephen Coulston^a

^a Department of Engineering, University of Exeter, Exeter

Version of record first published: 31 Aug 2006

To cite this article: Garry Lester & Stephen Coulston (2005): Liquid Crystal Filled Polymer Structure SLM Devices, *Molecular Crystals and Liquid Crystals*, 433:1, 117-127

To link to this article: <http://dx.doi.org/10.1080/15421400590957008>

PLEASE SCROLL DOWN FOR ARTICLE

Full terms and conditions of use: <http://www.tandfonline.com/page/terms-and-conditions>

This article may be used for research, teaching, and private study purposes. Any substantial or systematic reproduction, redistribution, reselling, loan, sub-licensing, systematic supply, or distribution in any form to anyone is expressly forbidden.

The publisher does not give any warranty express or implied or make any representation that the contents will be complete or accurate or up to date. The accuracy of any instructions, formulae, and drug doses should be independently verified with primary sources. The publisher shall not be liable for any loss, actions, claims, proceedings, demand, or costs or damages

whatsoever or howsoever caused arising directly or indirectly in connection with or arising out of the use of this material.

Liquid Crystal Filled Polymer Structure SLM Devices

Garry Lester
Stephen Coulston

Department of Engineering, University of Exeter, Exeter

Liquid Crystal Filled Polymer Structure (LiCFiPS) Devices consist of a polymer structure, which performs the desired spatial phase modulation of the incident light, filled with liquid crystal to permit modulation of this optical function. Fabrication of this type of device may be carried out at very low cost using established polymer embossing techniques. Devices with the liquid crystal aligned in the plane of the device and along the polymer faces have shown good quality optical switching. However regions with the liquid crystal aligned perpendicular to the grating lines show defects and inhomogeneities which give rise to spurious optical effects. To better understand the factors influencing the alignment of the liquid crystal computer modelling has been used to simulate the orientation of the liquid crystal director within such devices. The field within the device and orientation of the liquid crystal were calculated iteratively using the Landau-De Gennes form of the free-energy equation. The computational models of these devices show features that correspond well with the observed switching characteristics of actual devices. The features and changes that eradicate the defect provide insight into how the device configuration might be improved. While such devices might not offer the ultimate versatility of matrix addressed devices they do offer switchable optical devices of complex functions at very low cost.

Keywords: diffractive element; liquid crystal device; spatial light modulator; switchable gratings

INTRODUCTION

Liquid crystal filled polymer structure (LiCFiPS) devices potentially offer a low cost technology for fabrication of fixed function switchable spatial phase modulation devices. The devices are essentially a

The authors wish to thank the EPSRC for a studentship for Stephen Coulston. Thanks are also due to Dr Chris Newton and colleagues of HP-Labs Bristol for useful discussions while developing the computational model.

Address correspondence to Garry Lester, Department of Engineering, University of Exeter, North Park Road, Exeter, EX4 4QF. E-mail: g.a.lester@ex.ac.uk

polymer structure between two substrates each carrying transparent electrode coatings, the spaces in between being filled with liquid crystal. As the effective refractive index of the liquid crystal changes with applied field the refractive index, and therefore path length difference, between the polymer and liquid crystal regions gives rise to a controlled spatial phase modulation.

The polymer structure may be fabricated using hot embossing or similar techniques which lend themselves to low cost high volume production techniques developed for binary and multilevel diffractive devices [1]. This polymer structure fixes the spatial phase modulation to be applied to the transmitted optical wavefront, the change in effective refractive index of the liquid crystal filling is then used to modulate or switch this optical function. Though essentially fixed function devices LiCFiPS devices might be produced in volume using, for example, a continuous embossing roller process and therefore achieve very low unit cost indeed. In volume production the devices may be vacuum or capillary filled. Figure 1(a) and (b) show refractive and diffractive optical elements, the LiCFiPS construction is particularly well suited to binary diffractive optical elements such as dammann gratings.

There are other switchable optical component technologies [2,3,4], holographically formed polymer dispersed liquid crystal (HPDLC) type devices for example. LiCFiPS has the advantages of extremely low cost, ease of manufacture once the tooling has been made and drive voltages comparable to most LC display devices, a few volts. The PDLC type devices in comparison have driving voltage requirements of the order of tens or even hundreds of volts.

One of the main problems to be overcome in the liquid crystal device construction being considered here is that of achieving uniform liquid crystal alignment in the presence of the polymer structure's surfaces. Particularly, defects and non-uniformities have been observed to occur when the liquid crystal alignment direction is in conflict with the alignment of the liquid crystal on the polymer structure faces [5,6]. Binary optical devices have been tried to date [7,8] though the situation would be even more complex with multi-level devices. In this work a computational approach has been used to explore the device

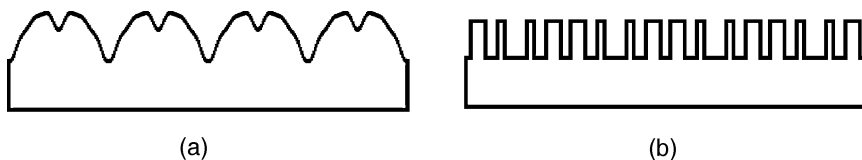


FIGURE 1 Continuous (a) and binary (b) optical elements.

parameters that give rise to the observed defects and this paper reports on one mechanism by which they may be suppressed, limiting the size of features between the structures.

DEVICE GEOMETRY AND COMPUTATIONAL MODELS

Device and Computational Geometry

The computational model was based on grating type devices with liquid crystal filled channels of MLC-6200-100 between walls of a polymer grating structure of SU8-2, both commercially available materials used in the previous experimental work. In this work the effect of the spacing between the polymer walls on the formation of the defect observed in grating devices [6] was investigated. The basic device geometry is illustrated in Figure 2, the main features of relevance to the liquid crystal director computation are the faces of the glass substrates and the surfaces of the polymer structure. In the real device these were rubbed Nylon on the upper substrate and the faces of the polymer SU8 structure, it was assumed that some SU8 remained at the bottom of the channel from the photolithographic process. In order to be comparable with earlier practical work the spacing between the two glass substrates was $6\mu\text{m}$ and the model was varied to give spacing between the polymer faces (the width of the liquid crystal filled channel) of between 5 and $50\mu\text{m}$. In order to more realistically model the real cell construction a liquid crystal filled gap of $0.5\mu\text{m}$ was also left between the top of the polymer and the upper glass substrate. Due to slight non-uniformities in the surface of spun-coated polymers such as SU8 there will be usually be some liquid crystal between the upper glass substrate and the top of the polymer structure. In the computational model repeating boundaries were applied so that the single computed channel was effectively part of an infinite grating. Also

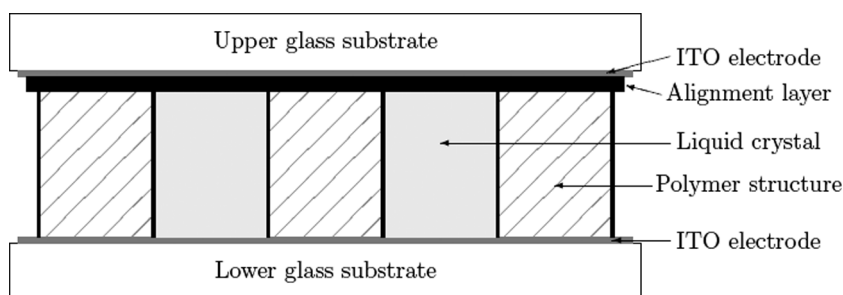


FIGURE 2 Liquid crystal filled polymer structure device cross-section.

repeating boundaries were applied to the model so that it represented an infinitely long liquid crystal filled channel.

Director Field Free Energy

The director profile in the different cell configurations were computed by minimisation of the free energy of the system. The Landau-de Gennes form of the free energy equation was used as the basis of the minimisation as it gives a more accurate representation of the director in systems that involve rapid changes in the director profile. The aim of this work was to investigate the formation of a defect, which necessarily exhibits rapid changes in the director orientation. The form of the bulk energy equation used in this work was [9]

$$f_b = \frac{k_{33} - k_{11} + 3k_{22}}{27} (Q_{jk}, lQ_{jk}, l) + \frac{2(k_{11} - k_{22})}{27} (Q_{jk}, lQ_{jk}, l) \\ + \frac{2(k_{33} - k_{11})}{27} (Q_{jk}, lQ_{jk}, l)$$

where Q_{jk} is the Q tensor

$$Q = \frac{S}{2} \left(3 \begin{bmatrix} n_x n_x & n_x n_y & n_z n_x \\ n_y n_x & n_y n_y & n_z n_y \\ n_z n_x & n_z n_y & n_z n_z \end{bmatrix} - \begin{vmatrix} 1 & 0 & 0 \\ 0 & 1 & 0 \\ 0 & 0 & 1 \end{vmatrix} \right)$$

In the actual devices a commercial liquid crystal MLC-6200-100 had been used, however the values of the elastic constants for this material were not readily available. For the computation, values of the physical parameters for a 'typical' liquid crystal were assumed in order to ascertain trends in the device characteristics with changes in the dimensions. The values for the elastic constants used in the bulk free energy calculation were $k_{11} = 14.4 \times 10^{-12}$, $k_{22} = 8.0 \times 10^{-12}$ and $k_{33} = 18.0 \times 10^{-12}$.

Modelling the Effect of Surface Interactions

The orientation of the liquid crystal in LiCFiPS devices is dominated by surface effects. Two main types of surface were considered in the computational model, linear and planar. For the rubbed polymer aligning surface on the upper substrate of the device there will be a tendency for the molecules to take up homogeneous alignment on the surface with a preferred direction of alignment, linear alignment. For the SU8 polymer structure surfaces there will be some tendency for the liquid crystal to take up homogenous alignment but with no

preferred direction on the surface, planar alignment. The Rapini-Papolar [12] anchoring energy expressions were used to give an energy term that was then included in the energy equation for the minimisation process.

For linear aligned surfaces this takes the form

$$f = \frac{1}{2} \frac{k}{L_s} \left(1 - (n \cdot n_s)^2 \right) \delta(P_i)$$

and for planar aligned surfaces takes the form

$$f = \frac{1}{2} \frac{k}{L_s} (n \cdot n_s)^2 \delta(P_i)$$

In these equations k is the average elastic constant for the liquid crystal and L_s is the correlation length of the surface modelled, $\delta(P_i)$ is a delta function that ensures that only the molecules adjacent to the surface i are affected by the surface and n is the direction of preferred alignment on that surface. For linear aligned surfaces this last term is the direction of preferred alignment, for planar surfaces this is the normal to the plane in which the molecules prefer to take up orientation.

For every liquid crystal mesh point in contact with a surface this gives an energy term that may be included in the free energy to be minimised. In the real devices the upper substrate was treated with rubbed Nylon as an aligning layer and it is known that L_s for Nylon is 40 nm [12]. The other surfaces in the device were all assumed to be SU8 polymer. It is believed from experimental observations that the anchoring strength of SU8 is relatively weak, so a value of $L_s = 400$ was used, considerably less than for Nylon.

Electric Field Computation

The defects in the real devices were observed to become much narrower with the application of an external electric field. To model the application of quasi-static electric fields the liquid crystal minimisation was carried out alternately with a finite difference approach to Laplacian E field calculation [10] where the potential at any one point in space is related to the potentials around it by [11]

$$V_p = \frac{\epsilon_x(V_{xp} + V_{xm}) + \epsilon_y(V_{yp} + V_{ym}) + \epsilon_z(V_{zp} + V_{zm})}{2(\epsilon_x + \epsilon_y + \epsilon_z)}$$

where V_p is the potential at point p and V_{xp} and V_{xm} are the potentials of the points in the 'plus' and 'minus' directions along the x axis from the point respectively. Applied iteratively the calculated potentials will

converge on the field distribution within the device. For the isotropic materials in the device such as the polymer $\epsilon_x = \epsilon_y = \epsilon_z$. In the liquid crystal region the effective values of the permittivity were obtained from the liquid crystal permittivities and the orientation of the liquid crystal, the director, at that point. The electric field energy to be included in the overall energy equation to be minimised was given by

$$f_e = \epsilon_0 \left[\Delta \epsilon (\vec{n} \cdot \vec{E})^2 + \epsilon_{\perp} \vec{E} \cdot \vec{E} \right]$$

There is an inherent coupling between the director and the electric field distribution as changes in the field will re-orient the liquid crystal and vice versa so the two had to be calculated alternately until the whole system had converged on a solution.

MODEL CALCULATIONS

Parallel and Perpendicular Grating

Initially as a test of the model it was attempted to reproduce the different observed liquid crystal alignments for devices with rubbing directions parallel and perpendicular to the liquid crystal channel (both in the plane of the glass substrates). Particularly the occurrence of the defect observed in perpendicular grating devices was expected. With the channel model described above a defect appeared in the computed director profile with similar conditions to the defect observed in real devices. As in the real device the defect in the computational model moved to one side, became narrower and finally disappeared with increasing field [6].

Dimensional Variation

Having established a model that successfully reproduced the observed defect structure the influence of the width of the liquid crystal region on the formation and stability of the defect was investigated, keeping the other parameters such as surface interactions and liquid crystal physical constants the same.

EFFECT OF LC CHANNEL SIZE

Range of Dimensions Explored

The range of widths of liquid crystal region explored in the grating model was $5\mu\text{m}$ up to $50\mu\text{m}$. This corresponds to the typical range

of feature sizes encountered in these devices. The practical lower limit is set partly by the SU8 photoresist in which it is problematic to make features significantly smaller than the order of $1\text{--}2\text{ }\mu\text{m}$. To allow direct comparison computations were carried out both for devices with the rubbing direction of the aligning surface along the grating channels and for devices with the rubbing direction perpendicular to the grating channels, the extremes of the alignment directions with respect to the polymer faces.

Observed Defects

The defects were seen to occur reproducibly in the larger devices and as in the real device the application of an electric field would sharpen the feature before it became extinguished. Figure 3 shows the director patterns for both sets of devices with an applied field of $1\text{V}/\mu\text{m}$. Clearly in the devices with larger liquid crystal filled spaces a defect line has formed and the application of an electric field has caused this to become sharper. However, at the smallest size investigated no defect formed and with application of an increased electric field uniform

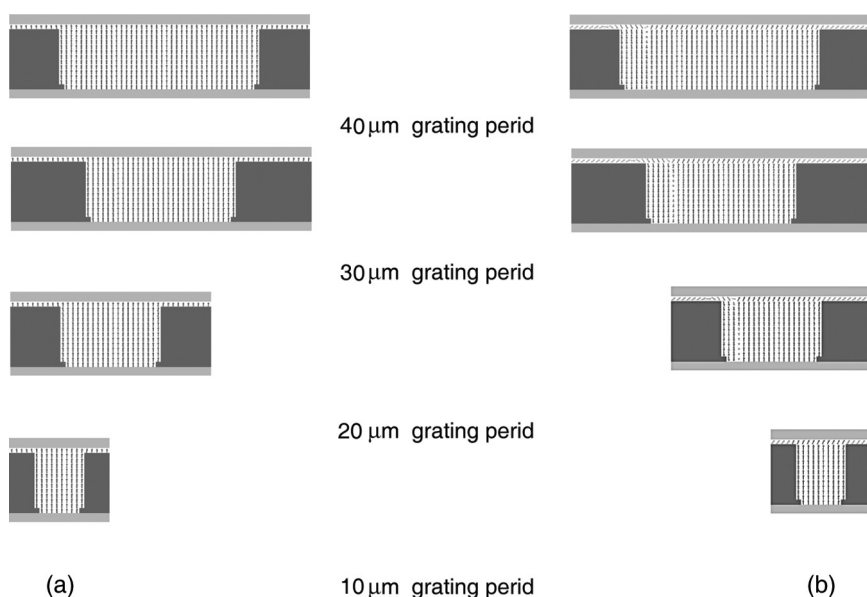


FIGURE 3 Computed director profiles in LiCFiPS devices with (a) rubbing direction along the LC channel and (b) rubbing direction perpendicular to the LC channel. (with $1\text{V}/\mu\text{m}$ electric field applied).

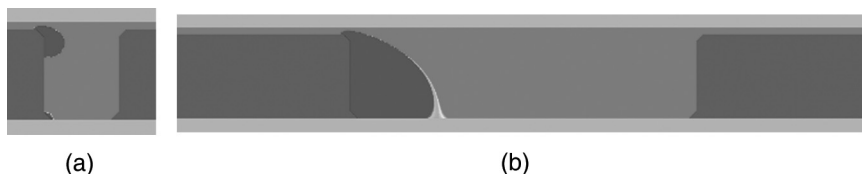


FIGURE 4 Component of the director along the liquid crystal channel (out of the plane of the page) showing defect pinning in the smaller devices.

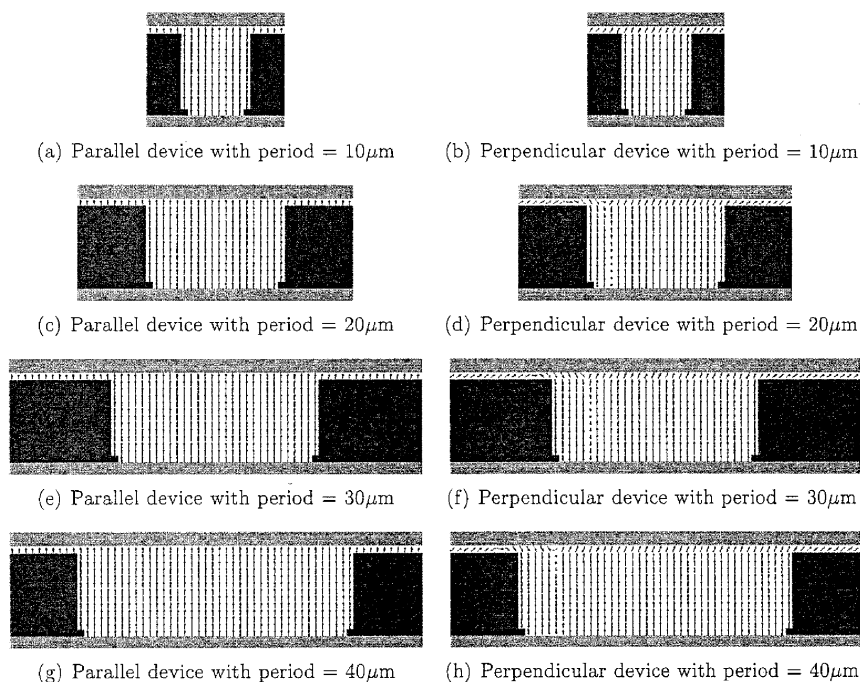
liquid crystal switching took place. This would imply that in devices with small features the formation of a defect is suppressed and good quality switching may be obtained.

To illustrate the differences in the director profiles for perpendicular aligned devices with different channel sizes Figure 4(a) and (b) show the variation of the components of the director up the device (from one substrate to the other). The effect of reducing the channel width until the surface forces from SU8 and the pretilt force the defect to become a small feature at one side of the grating are clearly visible.

EVALUATION

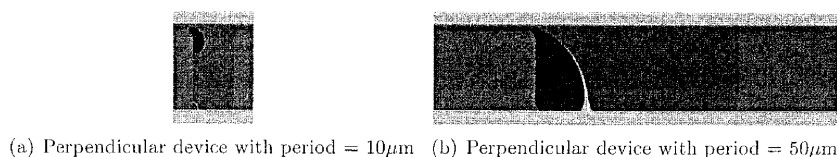
Liquid crystal filled polymer gratings with periods of a few tens of μm have been shown to work well when the liquid crystal is aligned along the grating channel but for more complex devices the alignment of the liquid crystal relative to the polymer structure will be more complex. In order to make more general switchable SLMs of good quality using the LiCFiPS approach it is essential to both understand and eradicate or control the occurrence of the defects in the liquid crystal region of the devices when the alignment is not simply related to that of the polymer structure.

From the absence of defect formation in a smaller liquid crystal channel with all other parameters remaining the same this would suggest that a holographic element with features limited in size would not exhibit liquid crystal defect formation and therefore show good quality switching. The size of the liquid crystal regions required for defect suppression is of a similar order to that required for the optical hologram [1]. For computer generated holograms the feature size might be put in as one of the constraints in the cost function used to generate the hologram. Further computational modelling work to understand in detail other parameters that may suppress the spurious alignment is the subject of ongoing investigation. For fabrication of practical devices it is likely that polymer structures made from materials other

**FIGURE 5**

than SU8 would be used. SU8 was used as a convenient and highly transparent photopolymer, however it has some problems when making small structures. This would not be a problem with embossed or similar polymer processing techniques.

One possible means of achieving good liquid crystal alignment within complex geometries has been identified even for cases when there is conflict between the rubbed surface and the polymer structure surfaces. For applications where the geometry of the polymer gives good alignment or the optical limitations imposed by the occurrence of defects is not of major concern the LiCFiPS devices offers several

**FIGURE 6**

advantages. Optically the devices provide a switchable spatial phase modulation and have therefore a high diffraction efficiency, though in most cases there will be a polarisation dependence in the optical function. The polymer structure may be produced at very low cost using embossing or similar production techniques and no photolithographic patterning of electrodes is required regardless of the complexity of the optical function to be implemented. As the polymer structure provides an extended spacer the devices are also extremely rugged. Using readily available materials low driving voltages of only a few volts are required for these devices.

CONCLUSION

Earlier work on LiCFiPs devices has demonstrated good quality switching in grating devices where there is no conflict of alignment between the polymer faces and the rubbed surfaces. For devices where this is not the case defects in the liquid crystal have been observed. This work has identified one possible solution to this, by limiting the size of the liquid crystal regions. This approach is likely to be a practical solution as features of appropriate dimensions are required in computer generated holograms and if necessary the feature size may be included as one of the constraints in the hologram computation.

REFERENCES

- [1] Herzig, H. P. (1997). Design of refractive and diffractive micro-optics', from micro-optics: Elements, systems and applications. In: Herzig, H. P. (Eds.), Taylor and Francis, 1–52.
- [2] Stalder, M. & Schadt, M. (1996). Beam steering devices based on switchable liquid crystal phase gratings, In: *Proc. of 16th Int. Disp. Res. Conf.*, Society for Information Display, Birmingham, 434–437.
- [3] McOwen, P. W., Gordon, M. S., & Hossak, W. J. (1993). A switchable liquid crystal Gabor lens. *Opt. Comms.*, 103, 189–193.
- [4] Chen, J., Bos, P. J., Vithana, H., & Johnson, D. L. (1995). An electro-optically controlled liquid crystal diffraction grating. *Appl. Phys. Lett.*, 67, 2588–2590.
- [5] Lester, G. A. & Strudwick, A. M. (2000). A liquid crystal phase grating for instrumentation applications. *J. Mod. Optics*, 47(11), 1959–1976.
- [6] Coulston, S. & Lester, G. (2004). Switching in liquid crystal filled polymer structures. *Mol. Cryst. Liq. Cryst.*, 413, 291–303.
- [7] Strudwick, A. M. & Lester, G. A. (1999). Electrically controlled phase grating for instrumentation applications. *Elec. Lett.*, 35(16), 1374–1375.
- [8] Lester, G. A. (2002). Optoelectronic devices for reconfigurable imaging and optical systems. In: *Recent Res. Devel. in Electronics*, Vol. 1, Trans World Research Network.

- [9] Li, W. Y. & Chen, S. H. (1999). Simluation of normal anchoring nematic droplets under electrical fields. *Jappanese Journal of Applied Physics*, 38, 1482–1487.
- [10] Hovaressian, S. A. & Pipes, L. A. (1969). *Digital Computer Methods in Engineering*, Mc Graw-Hill.
- [11] Desai, C. S. (1979). *Elementary Finite Element Method*, Prentice Hall, 299–332.
- [12] Newton, C. J., Iovane, M., Duhem, O., Barberi, R., Lombardo, G., & Spiller, T. P. Anchoring energy measurements: A practical approach. HPL Technical Reports, 200, 113, 1–11.